

We are IntechOpen, the world's leading publisher of Open Access books Built by scientists, for scientists

6,900

Open access books available

186,000

International authors and editors

200M

Downloads

Our authors are among the

154

Countries delivered to

TOP 1%

most cited scientists

12.2%

Contributors from top 500 universities



WEB OF SCIENCE™

Selection of our books indexed in the Book Citation Index
in Web of Science™ Core Collection (BKCI)

Interested in publishing with us?
Contact book.department@intechopen.com

Numbers displayed above are based on latest data collected.
For more information visit www.intechopen.com



Synthesis and Application of Porous Kaolin-Based ZSM-5 in the Petrochemical Industry

Ebrahim Mohiuddin, Yusuf Makarfi Isa, Masikana M. Mdleleni and David Key

Abstract

Zeolites are advanced chemical materials that play a significant role in many petrochemical applications. In recent years, research interest in improving and enhancing the effectiveness of ZSM-5 as a catalyst has grown immensely. In particular, finding cheaper, environmentally friendly alternative starting materials for the synthesis of ZSM-5 has gained much attention. Kaolin has been widely investigated as a zeolite precursor as it comprises the required constituents for an aluminosilicate zeolite material; ubiquitous nature and its benefit in synthesising zeolites are well known as an inexpensive way of obtaining catalysts. This chapter deals with the factors affecting ZSM-5 synthesis when utilising a kaolin precursor. The effects of kaolin crystallinity, kaolinite content and synthesis parameters on ZSM-5 formation and its physicochemical properties are discussed. The potential of kaolin-based ZSM-5 as an oligomerisation catalyst is investigated. Pure, crystalline ZSM-5 could be successfully synthesised from a kaolin precursor. Physicochemical properties such as morphology, porosity and acidity are affected by the kaolin precursor and optimum synthesis conditions are required for synthesis of ZSM-5 from particular kaolin. Kaolin-based ZSM-5 catalyst showed good activity and selectivity to valuable fuel range hydrocarbons.

Keywords: kaolin, ZSM-5, synthesis, oligomerisation, cracking

1. Introduction

Access to a variety of energy sources has been fundamental in driving human development. Fossil fuels have been a major source of energy for mankind for more than 5000 years. Today, crude oil continues to be a significant contributor to the energy sector; it accounts for a large percentage of the world's energy consumption. The production of chemicals has also continued to play a pivotal role in our daily activities. Interestingly, the amount of chemicals produced and used for both domestic and industrial purposes is very much related to the growth in global population. However, energy sources such as crude oil are non-renewable sources of fuel and current estimations show that world oil supplies will be depleted in the next century. Apart from the uncertainties in crude oil reserves, a major cause for concern is the impact crude oil extraction and its refining has on the environment; the combustion of fossil fuels leads to a net increase in greenhouse gases (GHG)

leading to global warming. These concerns among others have led researchers in the recent past to explore alternative energy sources to the traditional crude oil for the production of fuels and petrochemicals. Various practises such as the use of efficient catalysts and augmented reactor technology are currently being employed towards ensuring that production technologies are eco-friendly and sustainable.

Nanoporous materials are a large class of materials which consist of either an organic or inorganic framework structure containing ordered porous networks. They are generally classified by having pores sizes less than 100 nanometres and may be subdivided into three categories i.e. Microporous (<2 nm), Mesoporous (2–50 nm) and Macroporous (>50 nm). Their ability to interact or discriminate molecules depending on size has granted them scientific and technological importance. Research interest in nanoporous materials continues to grow as researches attempt to understand structure–property relations and design materials tailored for certain applications. Dependent on the properties of the nanoporous materials, applications range from purification and separation, sorption and drug delivery to energy storage, solar and fuel cells as well as electronic and magnetic devices. Typical examples include activated carbon, metal organic frameworks, ceramics, various polymers, aerogels, silicates and zeolites to name a few. Zeolites are microporous aluminosilicate materials that possess a 3-dimensional pore structure and play a prominent role in the petrochemical industry as ion exchangers, adsorbents, in separation and catalysis [1–4]. Their shape selective properties permit control of product distribution in chemical reactions and as such have become indispensable catalysts in many petrochemical processes [5]. Of particular importance to the petrochemical industry is zeolite ZSM-5. ZSM-5 because of its unique channel structure, acidity, and hydrothermal stability has been used as a shape selective catalyst in isomerization, alkylation, oligomerisation and catalytic cracking reactions [6–9]. It is conventionally synthesised using chemical sources such as sodium silicate solutions or silica gels and aluminium salts as the starting materials. Commercial synthetic zeolites are preferred over their naturally occurring analogues due to higher purity and uniform particle size which makes them more suitable for scientific and industrial applications [10]. However, zeolite synthesis using conventional methods leads to large amounts of waste being produced and chemical sources may be expensive, leading to high costs of zeolite production which limit commercialisation and use in many industrial applications [11]. Recently there have been increased efforts to explore the use of more affordable, natural raw materials possessing the necessary requirements for the synthesis of zeolites. ZSM-5 has been synthesised from natural silica and alumina sources such as rice husk ash [12–14], expanded perlite [15], palygorskite [16], fly ash [17], and kaolinite [18–21]. The main drive to utilise these rich aluminosilicate minerals is their relative abundances, cost effectiveness and overall more environmentally friendly synthetic procedures. Although many natural minerals and manufacturing wastes have been utilised to synthesise a wide variety of zeolite structures, this chapter will focus on kaolin-based ZSM-5 synthesis and possible application in the petrochemical industry.

Kaolin is a white clay composed mainly of kaolinite, a hydrous aluminosilicate mineral containing silica and alumina in a 1:1 ratio as well as impurities such as quartz and mica. Kaolin may require beneficiation to remove impurities depending on its application. Due to its low Si/Al ratio it has been extensively use in the synthesis of low silica zeolites [22, 23]. High silica zeolites such as ZSM-5 have also been synthesised with the addition of supplementary silica sources as well as through dealumination of kaolin via acid treatment [24–26]. Of the extensive range of aluminosilicate minerals used as zeolite precursors, kaolin has been favoured due to its ubiquitous nature. However, the studies of kaolin from different areas are significant since kaolin varies in composition depending on its geological occurrence. The chemical

compositions of materials affect their properties and variations in the kaolin structure and composition can thus affect its subsequent chemical reactivity [27, 28].

In this chapter the synthesis of kaolin-based ZSM-5 and the factors affecting synthesis are discussed. The work presented will focus on the synthesis of ZSM-5 using kaolin of South African origin. Most studies of kaolin derived ZSM-5 is performed on commercial kaolin. Only few have been done using raw kaolin. Chemical reactivities of kaolins obtained from different geological areas and the need to optimise synthesis conditions tailored to particular kaolin are highlighted. The effects of kaolinite content and synthesis parameters such as crystallisation time and temperature are discussed. The work is extended to include the effects of silica to alumina ratio on the physicochemical properties of ZSM-5 and is the main focus of this chapter. Furthermore, the application of kaolin-based ZSM-5 in important petrochemical processes such as the oligomerisation of olefins to fuel range hydrocarbons is evaluated.

2. Kaolin in zeolite synthesis

In the search for cheaper and more environmentally friendly alternatives to chemical sources, much research has been conducted on the feasibility of kaolin. By converting kaolin to the more reactive metakaolin via thermal activation and subjecting it to hydrothermal treatment in a NaOH medium, zeolite is produced. The use of kaolin as a source of silica and alumina was reported by Barrer [29] after it was calcined between 700 and 1000°C to form metakaolin. However due to the variations in kaolin composition and structure its subsequent chemical reactivity may be affected. Synthesis of zeolites from kaolin is affected by factors such as degree of crystallinity of the kaolin [23], kaolin composition [30], mineralogical impurities [23, 31], calcination temperature of kaolin [32], specific surface area of kaolin [33], synthesis parameters such as crystallisation temperature, time [30] and silica alumina ratio.

2.1 Factors affecting kaolin-based zeolite synthesis

2.1.1 Kaolin crystallinity

Many studies have been performed employing kaolin as the starting material for zeolite synthesis [34]. Investigations on the effects of kaolin crystallinity are contradictory as some researchers have shown that differences in the reaction kinetics of zeolite formation are observed for kaolin with different crystallinities or structural ordering [23] whereas others have reported that no significant differences were established when synthesising zeolites from kaolin of different crystallinity and reported that reactions of metakaolinites are independent of defects in the original crystal structure [22]. When two kaolins of South African origin from different geological areas i.e. Grahamstown (BK) and Fishoek (SK) were analysed it was shown that they differed in their structural order as well as composition and SK was more crystalline than BK [35]. The ZSM-5 synthesised using the two kaolin precursors resulted in differences in the crystallisation kinetics. The more disordered kaolin (BK) showed faster crystallisation kinetics than the more ordered SK. The physical and chemical properties of the reactive metakaolin of BK and SK were compared. The morphology obtained from SEM analysis shown that BK was composed of highly disordered loose kaolin plates compared to SK which possessed highly ordered stacked layers. The ordering remained even after calcination to form metakaolin. It was suggested that the highly disordered kaolin dissolved at a faster rate into the gel solution compared to SK in which the stacking layers were

preserved. The chemical properties of the kaolin samples were analysed using ^{27}Al and ^{29}Si NMR MAS spectroscopy. The different coordinations of aluminium and the relative amounts of each coordination type were correlated with the differences in reactivity of the two kaolins. These were determined for the kaolin before and after thermal activation, in the starting gels and products in order to observe the transformation of the Al environment as the zeolite was formed. After calcination of the precursors to form metakaolin, three distinct coordinations of Al i.e. tetrahedral (AlO_4), penta (AlO_5) and octahedral (AlO_6) species were observed however the relative amount of each differed between the two kaolins. The AlO_6 in kaolin was converted to more reactive AlO_5 and AlO_4 sites via dehydroxylation of kaolinite [36]. Metakaolin SK contained a larger amount of AlO_5 coordinated Al whereas metakaolin BK contained a larger amount of tetrahedrally coordinated Al at higher chemical shifts indicating the Aluminium existed in different environments of AlO_4 coordination. The peak occurring at higher chemical shift in ^{27}Al MAS NMR suggested the Al atoms are surrounded by different neighbouring atoms. Both q^4 and q^3 groups were identified. The q^4 group has 4 neighbouring Si atoms and the q^3 Al has 3 Si and 1 OH neighbouring group and is a highly reactive species [37]. It had been reported that metakaolins containing larger amounts of AlO_4 species due to metakaolinisation at the optimal thermal activation temperature showed increased chemical reactivity. The optimum thermal activation temperature however differed for kaolins of different structural order [38]. In the case of BK and SK the thermal activation temperatures were identical. Therefore, the results suggested that the amount of reactive q^3 AlO_4 species in particular may influence kaolin chemical reactivity and that chemical reactivity of the kaolin is indeed related to its crystallinity when thermally activated at the same temperature. ^{29}Si NMR also showed that Si atoms existed in different environments. Q^2 and Q^4 groups were identified. The Q^n groups refer to the number of neighbouring Si atoms [39, 40]. The relative amount of Q^2 and Q^4 groups showed that metakaolin of SK possessed more Q^4 (74%) species compared to metakaolin BK having more Q^2 (79%) species. This indicated that the Al and Si environments of BK and SK were different after calcination at the same temperature. The higher amount of neighbouring Si atoms in SK confirmed a higher degree of networking between Si atoms. This may therefore be related to a higher degree in structural order which may affect dissolution of metakaolin into the gel and the hence the crystallisation kinetics. When the dried gels of the zeolite batch mixtures were analysed by ^{29}Si NMR it was noticed that the gels were very similar and both exhibited a high degree of networking between Si atoms. However the ^{27}Al NMR differed as shown in **Figure 1**.

The dried gel spectra of BK and SK both show broad peaks in the tetrahedral coordination range with peak maxima at ~ 55 ppm corresponding to q^4 Al atoms. Dried gel BK however, possesses a shoulder peak at ~ 65 ppm indicating the presence of the reactive q^3 Al species. Therefore the q^3 Al from the calcined kaolin dissolves into the gel mixture and provides more reactive aluminium species to the starting gel of BK. The results also indicate that since the Si NMR spectra are similar the difference in chemical reactivity is mainly due to reactive alumina. The presence of the q^3 Al species may quickly form aluminosilicate species and govern the incorporation of Al into the framework and is most likely responsible for the faster crystallisation kinetics observed in ZSM-5 derived from BK.

The difference in crystallinity of kaolins and hence the difference in crystallisation kinetics leads to variations in the physicochemical properties of the zeolite. The synthesis parameters therefore have to be optimised to obtain a highly crystalline ZSM-5 zeolite. In this case for the more ordered SK a longer crystallisation time of 96 h compared to 48 h for BK was required to obtain a crystalline ZSM-5 with well-developed micropores. Furthermore, the acidic properties are also affected

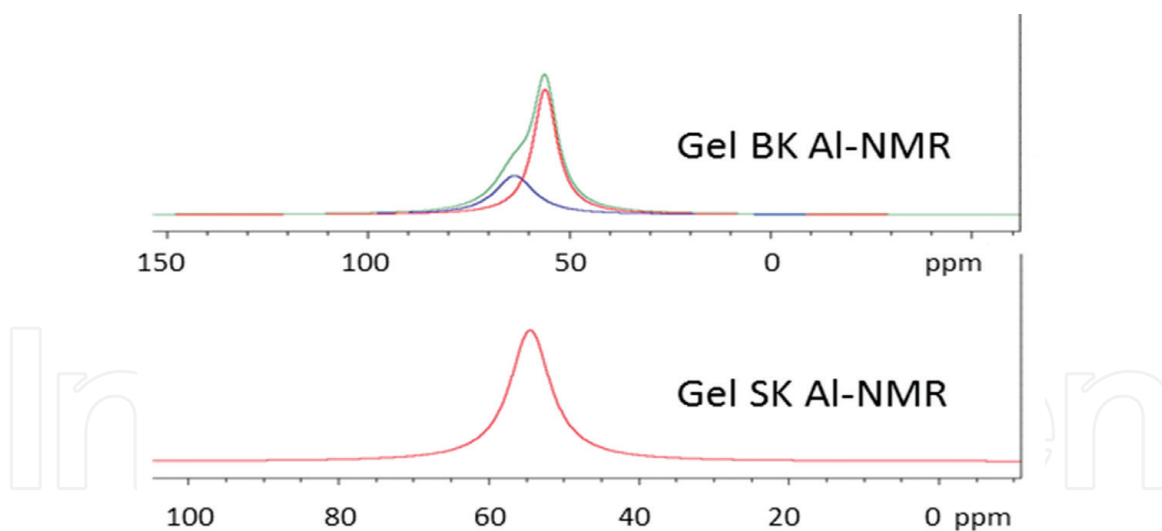


Figure 1. ²⁷Al MAS NMR spectra of dried gels of BK and SK showing the presence of different tetrahedral species [35].

and ZSM-5 was noticed to increase in acidity with an increase in crystallisation time when the more ordered SK was used a precursor.

2.1.2 Kaolinite content

The composition of kaolin varies greatly depending on its formation process and also can affect the chemistry of the clay. The clay comprises mainly kaolinite as well as impurities such as quartz, muscovite and feldspars. Other contaminants such as iron oxide and titania may also be present. The purity of kaolin determines its use in a range of applications. Kaolin if properly processed could be utilised in the production of whiteware ceramics, paper and filler pigment [41, 42] as well as in catalysis and cement production [43]. Highly contaminated kaolins such as those containing high amounts of iron oxide are used in the manufacture of bricks. While most studies have focused on the use of pure commercial kaolin in the synthesis of zeolites, only a few studies on the use of raw or virgin kaolins have been reported. Synthesis of ZSM-5 and zeolite A from kaolin of Nigerian origin containing a high amount of quartz has been reported [20, 44]. The respective zeolites could be synthesised after using beneficiation techniques (i.e. extensive settling and flocculation) or a modified autoclave to separate impurities from the synthesis gel. However, the ZSM-5 final product still contained quartz and mordenite impurities attributed to unreacted metakaolin and similarities in the synthesis conditions for both ZSM-5 and mordenite. The zeolite A purity was affected by colloidal impurities in the dispersion and the 'virgin' kaolin still required some treatment before use.

ZSM-5 was synthesised using highly impure kaolin with a high quartz content of large and finely grained quartz and muscovite originating from Grahamstown, South Africa [30]. Synthesis of ZSM-5 from raw (RK) and beneficiated kaolin (BK) was performed and the effect of the kaolinite content was investigated. Beneficiation was used to remove the majority of quartz and muscovite impurities and increase the kaolinite content. The composition of the kaolin was shown to play a significant effect on the formation of ZSM-5. From the beneficiated kaolin a highly pure crystalline ZSM-5 could be obtained. A higher kaolinite content results in more active silicate and aluminate species originating from the metakaolinite being present, which easily dissolve into the gel medium and form the primary building units necessary for nucleation and crystal growth in a shorter time period [21]. The results suggested higher kaolinite content shortens the induction period, increases the nucleation rate and hence the crystallisation of ZSM-5. However, from

the raw kaolin ZSM-5 could only be synthesised under optimum synthesis conditions i.e. crystallisation temperature and time which was established for the particular kaolin during the study. Even under optimum conditions ZSM-5 synthesised from RK still contained small quartz impurities. The quartz impurities are difficult to dissolve and are therefore undesirable in kaolin [45]. Substantial amounts of alumina may also be required when kaolin is used in zeolite synthesis [46]. Thus, utilising kaolin with low kaolinite contents (i.e. alumina source) and high quartz content may result in the hindrance of ZSM-5 formation under certain crystallisation conditions. Furthermore, the results from this study suggested that beneficiation is a necessary step for the synthesis of pure ZSM-5.

2.1.3 Crystallisation temperature and time

The synthesis parameters of crystallisation temperature and time are critical in controlling the phase purity of ZSM-5. Temperature is a major factor in the formation of zeolites due to its strong effects on nucleation and crystal growth [47]. The effect of crystallisation temperature on ZSM-5 formation from BK was studied by holding the crystallisation time constant at shorter (24 h) medium (48 h) and longer times (96 h) and varying the temperature from 120 to 190°C [30]. The XRD diffractograms showed a large amorphous peak corresponding to amorphous aluminosilicate in the gel mixture is present at 120°C. As the synthesis temperature was increased to 150°C the amorphous gel is converted into pure, crystalline ZSM-5 phase as the nucleation rate increased. At 190°C the metastable ZSM-5 re-dissolves into the gel and the intensity of the ZSM-5 peaks decreases as a more thermodynamically stable quartz phase crystallises. At a high temperature of 190°C zeolite synthesis follows the Ostwald's law of successive reactions. The initial metastable phase is replaced successively by more stable phases, in this case quartz. This trend is also observed at shorter and longer crystallisation times. Therefore at all crystallisation times studied, the optimum temperature for obtaining a highly crystalline pure ZSM-5 was determined to be 150°C. Similar results were reported by for the synthesis of ZSM-5 from Ahoko Nigerian Kaolin [48]. Although we might expect increased nucleation and crystal growth with an increase in temperature to 190°C, thermodynamic effects predominate over kinetic effects and favour the formation of the thermodynamically more stable quartz phase rather than growth of metastable ZSM-5 at 190°C.

Crystallisation time is critical in controlling the crystallinity of the synthesised ZSM-5. It was also shown to have a major impact on the physicochemical properties such as porosity and morphology of ZSM-5. The relative crystallinity determined from XRD increased with time at optimum crystallisation temperature of 150°C. SEM results showed different morphologies and crystal sizes could be obtained by varying the crystallisation times between 24 and 96 h. ZSM-5 with high external surface area and both micro and mesopores were obtained at 150°C 24 h using BK and that micro-pore area increased with time as the relative crystallinity increased. The studies on the effects of crystallisation temperature and time clearly highlighted the need to determine optimum synthesis conditions to obtain pure well crystallised ZSM-5.

2.1.4 SiO₂/Al₂O₃ ratio

In the synthesis of ZSM-5 the Si/Al ratio is known to affect physical properties such as crystal size and morphology as well as chemical properties such as acidity. The acid site density, type and strength are affected by the presence of aluminium and can be controlled by adjusting the Si/Al ratio. The acidity of the zeolite is

Zeolite	Atomic % Si	Atomic % Al	Si/Al ratio
Si-Al 150 RK	11.67	0.30	39.0
Si-Al 70 RK	97.2	2.77	35.1
Si-Al 42 RK	91.51	6.48	14.1
Si-Al 150 BK	11.97	0.30	39.9
Si-Al 70 BK	42.18	2.51	16.8
Si-Al 42 BK	37.2	5.04	7.4

Table 1.
 EDS results showing atomic composition (%) of synthesised ZSM-5 with different Si/Al ratios using RK and BK.

important as ZSM-5 is used in many acid catalysed petrochemical reactions such as oligomerisation of olefins, cracking, isomerisation and alkylation. In this study the Si/Al ratios were varied and its effects on the physicochemical properties of the ZSM-5 are investigated. Raw kaolin (RK) and beneficiated kaolin (BK) are used as alumina source. The study shows the effects of the kaolin compositions when the Si/Al ratios are varied on the formation and properties of the zeolites. The ZSM-5 zeolites were synthesised using RK and BK with molar SiO₂/Al₂O₃ ratios of 150, 70 and 42 in the batch mixture. The Si/Al ratios in the final product were determined using EDS atomic analysis. (It must be noted that the term Si/Al is used interchangeably but SiO₂/Al₂O₃ is meant when referring to the batch ratio and Si/Al is meant when referring to the ratio in the product as determined by EDS analysis.) The atomic percentages of Si and Al are shown in **Table 1**.

The Si/Al ratios of the final ZSM-5 product decrease as the initial Si/Al ratios in the batch mixtures decrease for both RK and BK. The Si/Al ratios of ZSM-5 synthesised from batch mixtures 70 and 42 BK are lower, approximately half that synthesised from RK of the same starting ratios respectively. This suggests that as the Si/Al ratio decreases less silica may be incorporated into ZSM-5 formed from BK compared to RK.

The effect of Si/Al ratio on the structure of ZSM-5 was confirmed by x-ray diffraction. The diffractograms are shown in **Figure 2(a)** and **(b)**. All patterns exhibited the characteristic ZSM-5 peaks at 7.94° (011), 8.90° (020), 23.10° (051), 24.0° (033) and 24.35° (313) 2θ. All samples synthesised from RK also showed a reflection at 26.67° 2θ corresponding to the presence of quartz. The intensity of this peak

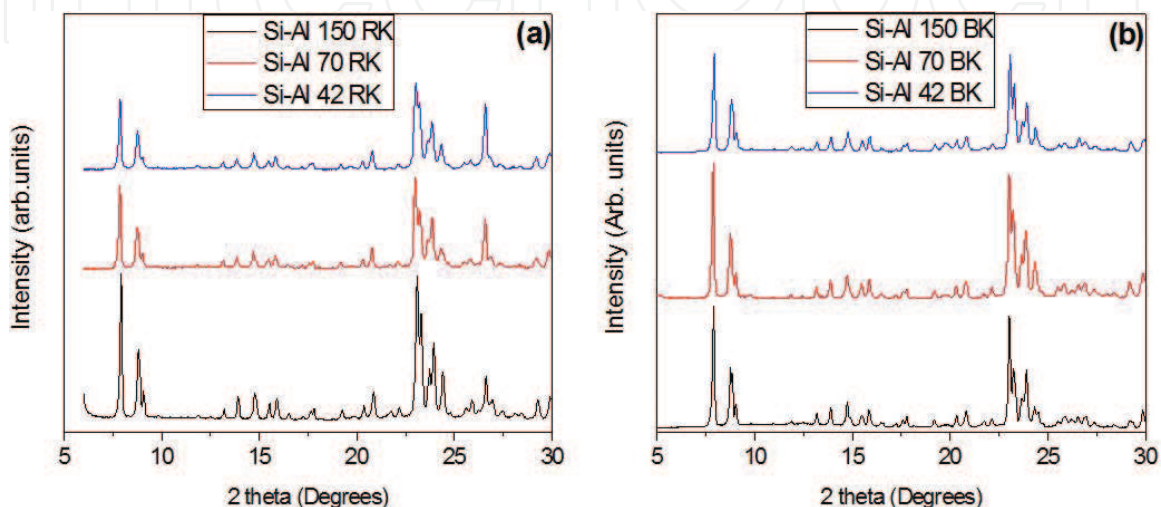


Figure 2.
 XRD powder patterns of ZSM-5 synthesised from (a) RK and (b) BK with different Si/Al ratios.

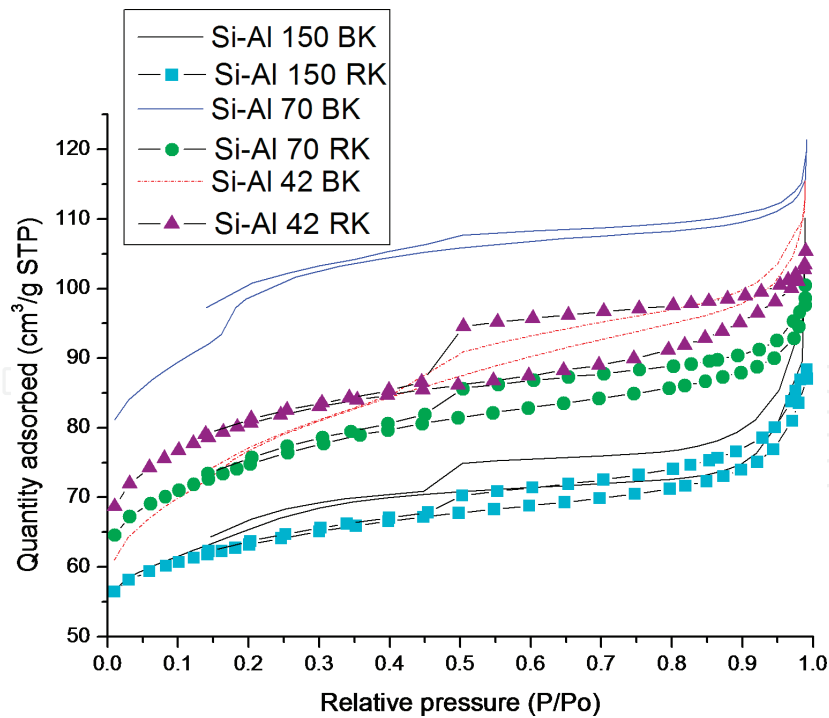


Figure 3.
N₂ adsorption-desorption isotherms of the representative samples.

increased as the Si/Al ratio decreased. RK used as the aluminium source contains a significant amount of quartz. Samples synthesised with lower Si/Al ratios thus contained a larger amount of quartz which remained unreacted hence the increase in intensity of the quartz phase. As the Si/Al ratio in the RK samples decreased the intensity of the (011) and (020) reflections diminished and peaks shifted to slightly lower angles. This is due to a change in the crystal size and an increase in Al substitution in the framework structure. Peak intensity however increased from sample Si-Al 150 BK to Si-Al 70 BK as the material became more crystalline but then decreased in sample Si-Al 42 BK.

The specific surface area and porosity characteristics of the samples are shown in **Table 2** and N₂ adsorption-desorption isotherms in **Figure 3**. From **Table 2** it is noticed that the specific surface area increases as the Si/Al ratio decreases for the RK samples. The micropore, external surface area as well as the micropore volume increase as the Si/Al ratio decreases.

Zeolite	BET s/a m ² /g	Micropore area m ² /g	External area m ² /g	Avg. pore vol. m ³ /g	Micropore vol. m ³ /g	Avg. pore size nm
Si-Al 150 RK	214	159	55	0.125	0.073	5.8
Si-Al 70 RK	253	171	82	0.143	0.079	4.6
Si-Al 42 RK	274	189	85	0.155	0.087	4.8
Si-Al 150 BK	223	137	86	0.133	0.063	6.8
Si-Al 70 BK	340	162	178	0.174	0.072	3.1
Si-Al 42 BK	265	121	144	0.162	0.055	4.2

Table 2.
Specific surface area and porosity characteristics of RK and BK samples with different Si/Al ratios.

This indicates that the increase in aluminium content in the samples leads to a well-developed internal microporous structure. The increase in external surface area with lower Si/Al ratios is likely due to the decrease in crystal size and correlates with the decreased intensity of the XRD reflections. The presence of more quartz as the Si/Al ratio decrease may also result in a higher external surface area. All samples possess a type 1 adsorption isotherm indicative of the microporous nature of the synthesised ZSM-5. The samples also exhibit a H4 type hysteresis loop in the relative partial pressure range 0.4–1.0, indicating capillary condensation occurred. This has been attributed to the presence of a mesoporous phase associated with the slit shaped voids between packed crystals [49]. A large uptake in the P/P_0 range 0.9–1.0 suggests the presence of larger macropores. This however decreases with decrease in Si/Al ratio. The hysteresis loop becomes wider as the Si/Al ratio decreases. Similar results have been shown by Liu et al. [50] for ZSM-5 synthesised from gel mixtures of varying polymerisation degrees. The more depolymerised gel formed uniform aggregates of fine crystals. Therefore as the Si/Al ratio decreased the gel became more depolymerized forming aggregates of tiny crystals which when tightly packed form mesopores between them [51]. Si-Al 42 RK also showed a broad peak centred at approximately 12.4 nm in the pore size distribution curves shown in **Figure 4(a)** not seen in the other RK samples which is indicative of mesopores and hence the broader hysteresis loop. Samples from BK had a lower micropore area and volume and higher external surface area compared to those synthesised from RK. The crystallisation process is different when using RK and BK as the compositions differ. This may suggest a difference in the degree of polymerisation of silica and alumina in RK and BK. As suggested, the N_2 isotherms and SEM images confirm the presence of aggregated nanocrystals in RK samples which form well depolymerized gel mixtures forming tetrahedral silica and alumina building blocks that form highly networked aluminosilicate species leading to a highly crystalline microporous structure. Zhang et al. [52] suggests a destruction of the microporous structure of ZSM-5 occurs with isomorphous substitution of Si with Al. This is possible as there is a higher content of aluminium in the BK samples compared to RK for each particular ratio. It is more likely however that extra-framework aluminium is present which blocks the micropores since Si-Al 70 BK has a higher micropore area and volume than Si-Al 150 BK but Si-Al 42 BK containing the highest aluminium content has the lowest microporosity. Therefore there is an optimum Si/Al ratio

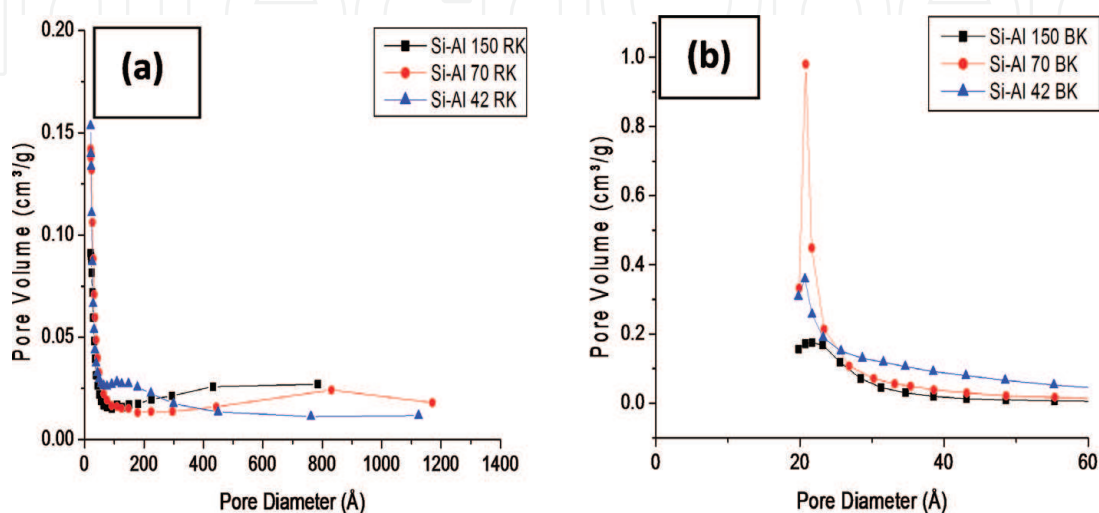


Figure 4. Pore size distribution calculated using the BJH method for the representative samples synthesised from (a) RK and (b) BK.

when synthesising ZSM-5 using BK. Interesting to note is the shape of the Si-Al 70 BK isotherms. It is a combination of a type I isotherm typical of ZSM-5 with a microporous framework and a type IV isotherm representative of mesoporous materials. The hysteresis loop in the 0.4–1.0 P/P_0 range is much smaller than other samples probably due to less space between packed crystals. However, the steep uptake at approximately 0.2 P/P_0 with a second small hysteresis loop may be due to the presence of uniform pores in the 2 nm range as shown in the pore size distribution graph for BK samples in **Figure 4(b)**. Isotherms of this type have been reported in the literature for hierarchical zeolites [49, 53–55] and are ascribed to filling of mesopores with a narrow pore size distribution between 3 and 4 nm. The pore size in this sample is smaller and similar to the size of supermicropores described by Yang et al. [56]. From **Figure 4(b)** it is noticed that the presence of 2 nm sized pores increase with decreasing Si-Al ratio and exist even for Si-Al 42 BK which has the lowest Si-Al ratio although the amount decreased probably due to the blockage of pores by extra-framework aluminium. We consider that these are real pores and not physical phenomena observed in gas adsorption such as fluid to crystalline transitions observed in MFI zeolite structures on the basis that Si-Al 70 BK has a low Si/Al ratio. Fluid to crystalline effects are usually observed on high Si/Al ratio MFI and silicalite-1 materials due to the energetically homogenous surface created by the large amount of Si atoms which result in a well-pronounced sub-step in a narrow P/P_0 range and an increase in Al content induces energetic heterogeneity [57].

HRSEM studies revealed that the morphology and particle size is affected by the change in Si/Al ratio. The images for the RK and BK samples are shown in **Figure 5**. Si-Al 150 RK has rounded boat shaped crystals that are highly inter-grown and agglomerated. There is also the presence of some amorphous material with no particular morphology.

As the Si/Al ratio decreases the crystal size also decreases as shown in **Figure 5(a–c)**. This agrees well with results reported in literature [24] and correlates with the increase in surface area and decrease of intensity of reflections as shown by BET and XRD results respectively. The material also becomes less inter-grown and aggregates with a uniform size distribution are noticed. Looking at the insets of **Figure 5(b) and (c)** it can be clearly seen that the aggregates are made up of nano-sized crystals that interlock and form an overall cross discus shape. ZSM-5 with similar morphology has been synthesised by Yue et al. [58] in the synthesis of hierarchical zeolites from kaolin and rectorite using a nanoscale depolymerisation-reorganisation approach and by Liu et al. [50] from highly depolymerised gel mixtures which also show similar trends in gas adsorption analysis to our samples. Thus an explanation of the change in morphology to aggregates of nano-crystals with a decrease in Si/Al ratio is that the gel mixture becomes more depolymerised with increased amount of the aluminium source. This trend is only observed in RK samples and not BK. The formation of the aggregates is due to the difference in composition of RK and BK in which the former contains a high quantity of quartz. As the aluminium amount is increased to obtain lower Si/Al ratios the quartz content in the gel mixture also increases and is present as shown in XRD. The quartz is difficult to dissolve which means that the alkalinity may be higher for the more soluble species i.e. that obtained from kaolinite and additional water-glass which is readily consumed. As crystallisation proceeds it becomes more depolymerized and leads to formation of fine crystals [50].

Si-Al 150 BK had larger crystals than Si-Al 70 and 42 BK and followed the trend of decreasing crystal size with lower Si/Al ratios. As noticed in **Figure 5(d)** the morphology is hexagonally shaped crystals. Twinning is also apparent as the 100 face protrudes from the 010 face and is commonly seen in ZSM-5 crystal twinning.

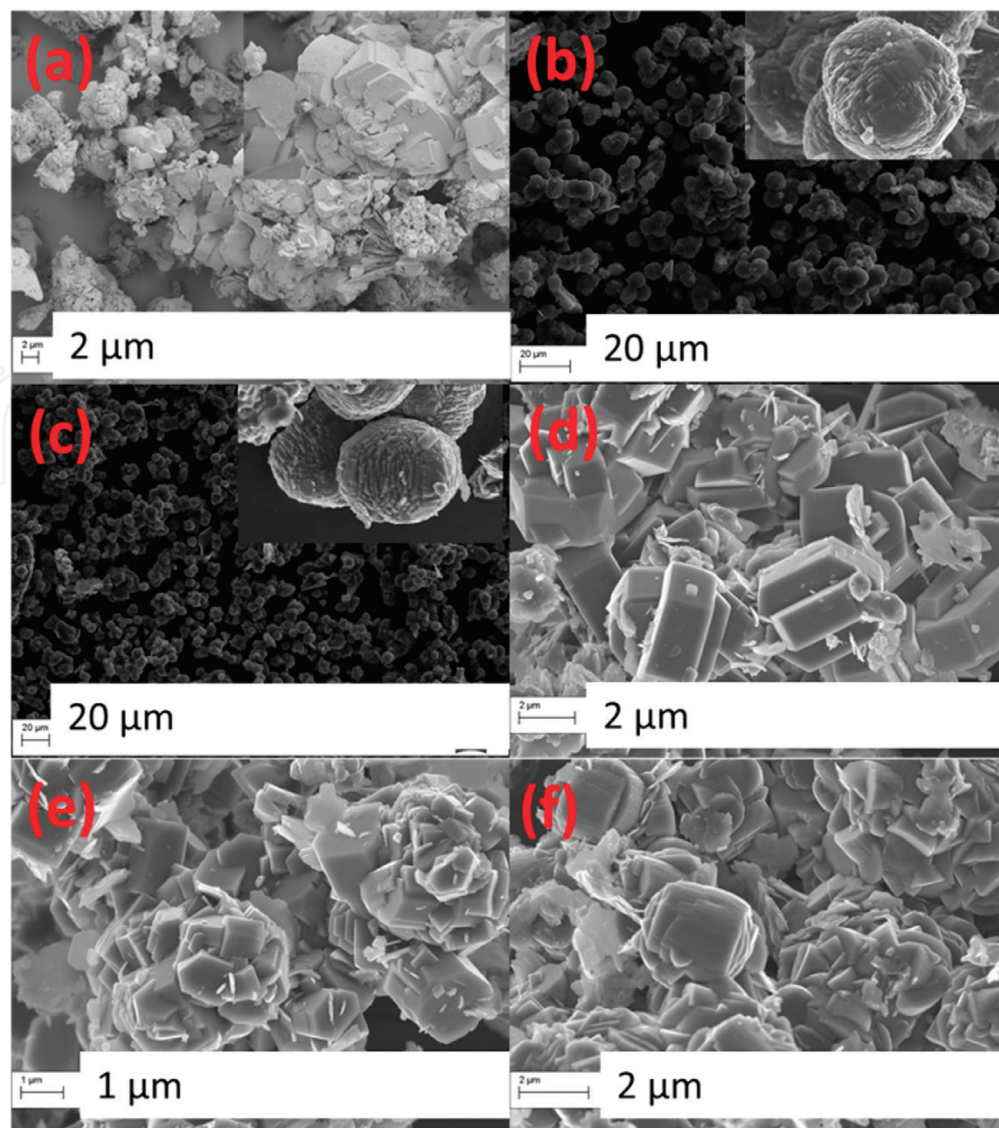


Figure 5. High resolution SEM images showing morphology and crystal size of (a) Si-Al 150 RK, (b) Si-Al 70 RK, (c) Si-Al 42 RK, (d) Si-Al 150 BK, (e) Si-Al 70 BK and (f) Si-Al 42 BK.

Si-Al 70 BK and Si-Al 42 BK both have wide crystal size distributions of both micrometre and sub-micrometre crystals that are highly intergrown with the former possessing smooth hexagonal crystals and the latter more rounded and rough edged crystals. Thus the Si/Al ratio also has an effect on morphology which agrees with work that has been reported in the literature [24].

The amount and strength of acid sites were determined by the NH_3 detected during desorption and the peak maximum in the desorption profile respectively. The results are summarised in **Table 3**.

It is clearly seen from **Table 3** that the total amount of acid sites increase with decreasing Si/Al ratio for RK samples as the higher the Si/Al ratio the lesser amount of total acid sites is [59]. This is true for the BK samples with the exception of Si/Al 42 BK which has the lowest Si/Al ratio but has lesser amount of acid sites than Si-Al 70 BK. This is most likely due to a larger amount of extra-framework aluminium and thus less Bronsted acid sites. This is supported by the fact that it has the least amount of strong acid sites ($206 \mu\text{mol/g}$), which are mainly due to NH_3 desorption from Bronsted sites. The decrease in the amount and strength of acid sites when a batch ratio of 42 is used may be due to the aluminium atom being in close proximity to each other forming Al pairs which reduce the amount of acid sites. Both the amounts of weak and strong acid sites in general increase with decreasing Si/Al

Samples	Peak (°C)		Acidity distribution ($\mu\text{mol NH}_3/\text{g}$)		
	Low temp	High temp	Weak	Strong	Total
Si-Al 150 RK	191	395	230	225	455
Si-Al 70 RK	192	408	269	279	548
Si-Al 42 RK	200	421	536	500	1036
Si-Al 150 BK	200	413	354	279	633
Si-Al 70 BK	210	440	689	519	1208
Si-Al 42 BK	203	423	584	206	790

Table 3. Distribution of acidity on the ZSM-5 samples as determined by NH_3 -TPD.

ratio. The RK samples have an almost 1:1 ratio of weak and strong acid sites. The BK samples however possess more weak acid sites than strong ones which may be due to NH_3 desorption from the silanols caused by the defects in the crystalline structure. The strength of the acid sites varies with aluminium content and seems to increase with decreasing Si/Al ratio. The maxima of the peaks shift with decreasing Si/Al ratio to higher temperatures indicating that the NH_3 molecule is more strongly bound to the acid sites. The maximum peak temperatures as shown in **Table 3** indicate that ZSM-5 synthesised from BK have stronger acid sites when compared to those synthesised from RK with similar aluminium content. This may be due to the difference in aluminium environment as those synthesised from RK are more crystalline whereas those synthesised from BK contain more defects.

It is well known that the aluminium content is directly related to the acidic properties of aluminosilicates. The presence of different Al species or coordination types leads to the formation of both Bronsted and Lewis acid sites. Therefore ZSM-5 samples with different Si/Al ratios synthesised from RK and BK were studied in order to determine the aluminium state, coordination, stability and degree of incorporation. The data obtained from ^{27}Al MAS NMR investigations are presented in **Table 4**.

Two peaks are commonly noticed in the ^{27}Al NMR spectra of ZSM-5 zeolites. The major peak occurring at a chemical shift of approximately 55 ppm corresponding to the tetrahedrally coordinated Al in the zeolite framework and another smaller peak at approximately 0 ppm is related to the presence of octahedrally coordinated Al and is usually referred to as extra-framework aluminium [60]. This notion has been disputed, however, as evidence for octahedrally coordinated Lewis Al present

Sample	Al framework (% Al_{fr})	Al extra-framework (% Al_{efr})	PW at 1/2 max (~55 ppm Al_{fr})
Si-Al 150 RK	100	n.d	4.9
Si-Al 70 RK	92	8	5.5
Si-Al 42 RK	92	8	5.7
Si-Al 150 BK	93	7	5.3
Si-Al 70 BK	89	11	5.8
Si-Al 42 BK	83	17	5.6

Table 4. Framework and extra-framework Al contents and line widths at half height for the representative ZSM-5 samples.

as $\text{Al}-(\text{OSi})_3(\text{H}_2\text{O})_3$ in the framework has been confirmed by Woolery et al. [61]. The relative amounts of the two species have been obtained by integration of the two peaks and are shown in **Table 4**. It is noticed that Si-Al 150 RK contains only tetrahedrally coordinated framework aluminium (Al_{fr}) and any presence of extra-framework aluminium (Al_{efr}) is negligible. It is common for highly siliceous ZSM-5 to possess only Al_{fr} . Si-Al 150 BK which has a similar Si-Al ratio as Si-Al 150 RK as shown in **Table 1** does have a small amount of Al_{efr} . This may be due to the difference in the composition and hence solubility of RK and BK. A slight increase in Al_{efr} is seen as the aluminium content increases for RK samples although there is not much difference between Si-Al 70 and Si-Al 42 RK. The increase in Al_{efr} with increase in aluminium content however, is drastically enhanced for the BK samples. EDS analysis shows that Al content is almost double in Si-Al 70 and Si-Al 42 BK compared to that synthesised from RK with the same starting gel ratios confirming that more Al is incorporated into ZSM-5 from BK due to a more abundant supply of reactive aluminium. However, NMR suggests that the Al is not necessarily all in framework positions and Al available from RK is better incorporated into the framework structure as it has a greater amount (92%) compared to Si-Al 70 BK and Si-Al 42 BK only having 89 and 83% Al_{fr} respectively. This result correlates with that obtained from N_2 physisorption and SEM analysis which showed a larger micropore area and nano crystal aggregates respectively for the RK samples compared to BK. This suggests a well-structured crystalline material made up of tetrahedrally coordinated Si and Al. It must be noted that quantitatively the BK samples form more Al-rich ZSM-5 even though the Al_{efr} amounts are greater. BK samples had a large external surface area greater than its micropore area due to mesoporosity. Larger amounts of aluminium may therefore be present at the external surface of the zeolite in a less stable octahedral form as suggested by Serrano et al. [53] for materials with more than 1 type of porosity such as hierarchical zeolites. They may also be present in different environments with more than 1 type of neighbouring atom as the resonances observed are broad and Si-Al 42 BK also shows a shoulder peak at ~6 ppm as shown in **Figure 6**.

From the ^{27}Al NMR spectra of the RK and BK samples, The RK samples and Si-Al 150 BK all have a peak max at ~55.7 ppm. Si-Al 70 BK shows a slight shift to a lower value ~54 ppm and Si-Al 42 BK a larger shift to ~58.3 ppm. The peak width values shown in **Table 4** are an indication of the uniformity of the Al environments in zeolite materials [53, 62] and crystallinity [63]. Si-Al 150 RK has the smallest peak width indicating high crystallinity and correlates with the XRD results and a more uniform Al environment. The peak width increases for all other samples indicating different environments of Al. The base of the peak begins at ~50 ppm and ends at ~62 ppm for all samples except Si-Al 42 BK which shows a shift of approximately ~4 ppm towards higher ppm values. Previous studies by Dedecek et al. [37] have shown that different environments for AlO_4 tetrahedra exist after deconvolution and simulation of the tetrahedral peak. Peaks observed at 50, 53, and 58 ppm correspond to Al atoms with only Si neighbours, while resonances at 62 ppm corresponds to Al atoms with 3 Si and 1 neighbouring OH group which are highly reactive. Thus the resonances fall within the range of the peak observed for the ZSM-5 samples. The resonances at 50, 53 and 58 ppm reflect the difference in environment of the AlO_4 tetrahedra in the sample which is due to the effect of the vicinity of second Al atom in the sample [37]. The closeness of the next Al atom in sequences such as $\text{Al}-\text{O}-(\text{Si}-\text{O})_2-\text{Al}$ can change the observed shift of the Al atom by ~4 ppm. Thus the peak observed for Si-Al 42 BK at 58.3 ppm suggests that the Al atoms are in close proximity to each other and has been reported for Al rich zeolites [37, 64]. Si-Al 42 BK also more likely has more Al atoms with a neighbouring OH which are highly reactive as the resonance shifts towards 62 ppm. Therefore it is

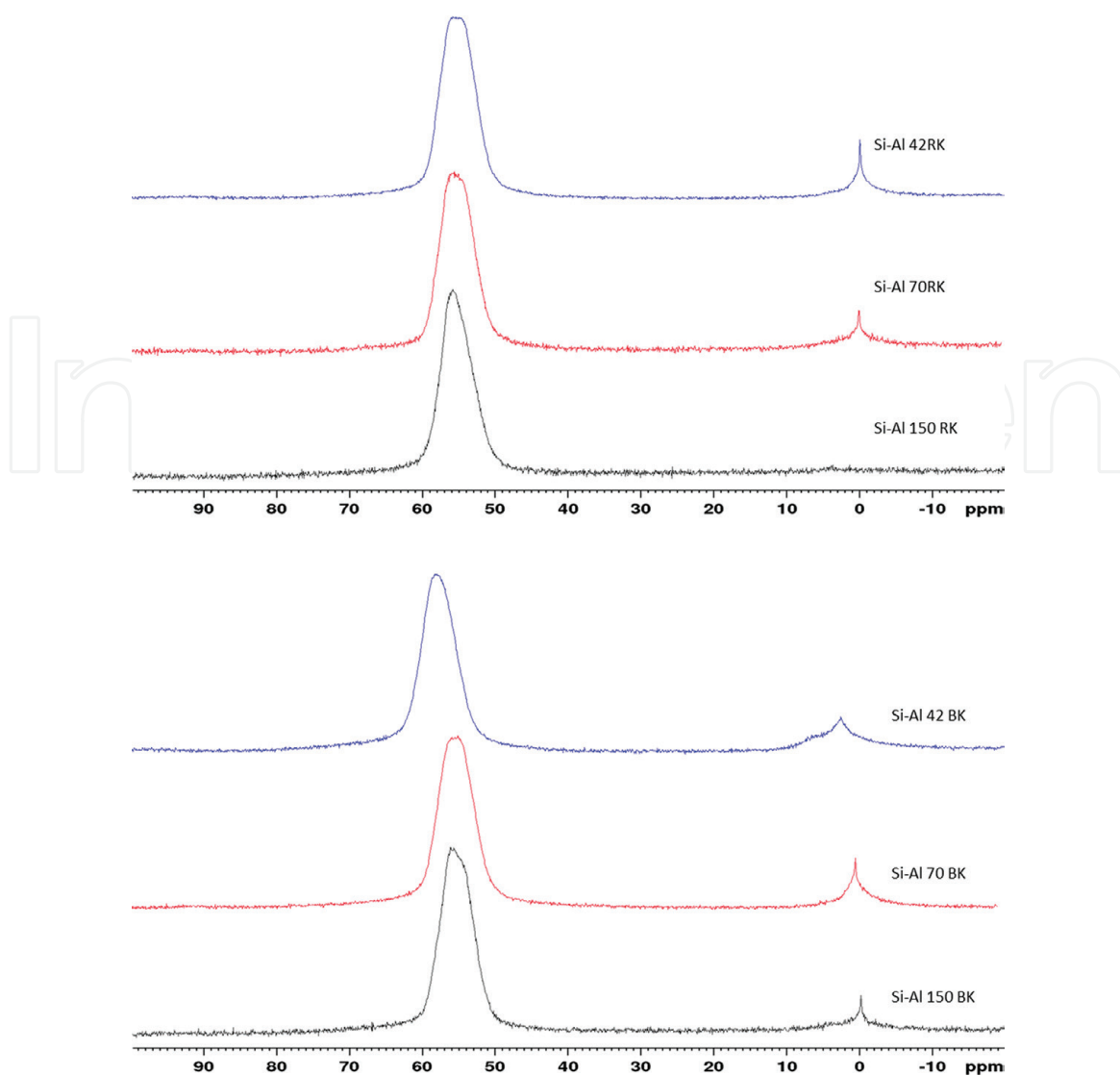


Figure 6.
²⁷Al MAS NMR spectra of the RK and BK samples with different Si/Al ratios.

possible that BK forms more Al rich ZSM-5 than RK for two reasons. The first being that RK causes a higher degree of depolymerisation due to the presence of quartz (as discussed above) of the remaining Na-silicate which is broken down to silicate species. This then forms more networked silicate and aluminosilicate and has less formation of close Al atoms resulting in higher ratios. Second for the BK samples, which were prepared with a smaller amount of additional Na-silicate, was not well depolymerised due to a lower alkalinity i.e. the silicate remained non-transformed and balanced by the Na⁺ and only a much lower concentration of Si was available for the highly reactive Al species resulting in aluminosilicate with a much lower Si/Al ratio having also more Al_{efr} and in the case of Si-Al 42 BK, in a high probability of aluminosilicate species with close Al atoms [37].

3. Potential application of kaolin-based ZSM-5

3.1 Catalytic oligomerisation

The performance of the zeolites as catalysts was tested in the transformation of 1-hexene, used as a model compound for the oligomerisation of alkenes; reaction was performed at the following conditions: T = 350°C, pressure = 1 atm, WHSV = 8 h⁻¹. The activities of the catalysts were determined by assuming all

1-hexene present in the product was due to unconverted feed. The graph showing activity as a function of time on stream is shown in **Figure 7**.

The catalytic tests were conducted over a time period of 420 min. All catalysts showed some deactivation over the total time on stream although some were more rapidly deactivated than others. All catalysts had a conversion not less than 90% in the first hour on stream. The highest conversion achieved was approximately 98%. It is clearly noticed that the conversion of the catalysts is highly dependent on the acidity, in particular the Bronsted acidity. Si-Al 42 RK and Si-Al 70 BK with similar acidities and possessing the highest acidities of the catalysts had the highest conversions and both showed only slight deactivation as the conversion remained above 90% for the duration of the reaction. Si-Al 70 RK and Si-Al 150 BK having identical amounts of strong acid sites and tetrahedral alumina (**Tables 3** and **4** respectively) have the same conversion and deactivation for the time on stream. Si-Al 42 BK which had the least amount of Bronsted sites showed the lowest conversion and the most rapid deactivation. Interestingly, Si-Al 150 RK having a much lower acidity compared to Si-Al 42 RK and Si-Al 70 BK has a very similar activity and shows even better stability (**Figure 7**). This was attributed to the effect of quartz coating the surface of the ZSM-5 which prevents deactivation. Therefore it is seen that this catalyst functions better than catalysts with more than double its acidity and further validates the influence of quartz on the performance of the catalyst.

The catalysts tested in the transformation of 1-hexene all possess a wide product distribution. The products are grouped accordingly: (C_2-C_5) range, (C_6-C_9) gasoline range and (C_{10+}) diesel range. This indicates multiple types of reactions may occur at the set reaction conditions such as oligomerisation, cracking, isomerisation and alkylation to name a few. The selectivities to these ranges however change with time on stream and it is noticed that small changes in conversion can have large changes in selectivity to products. The selectivities of the catalysts are discussed further and correlated with their physicochemical properties.

Si-Al 150 BK and Si-Al 70 RK are compared to each other since they have similar acidities as well as conversions over time on stream as shown in **Figure 7**. The selectivities however differ from each other. The selectivities to gasoline (C_6-C_9) and diesel (C_{10+}) ranges are shown in **Figure 8(a)** and **(b)** respectively.

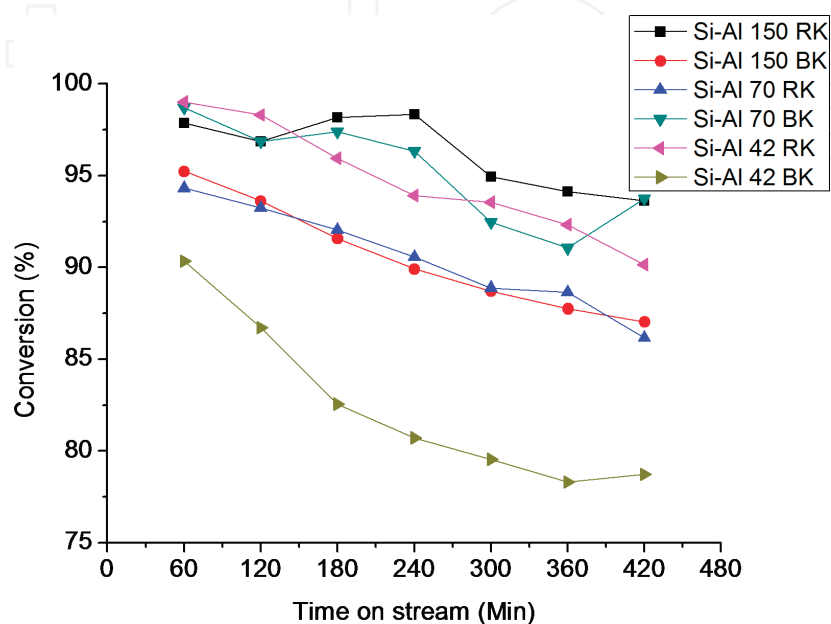


Figure 7. Graph showing hexane conversion over different catalysts ($P = 1 \text{ atm}$, $T = 350^\circ\text{C}$, $\text{WHSV} = 8 \text{ h}^{-1}$).

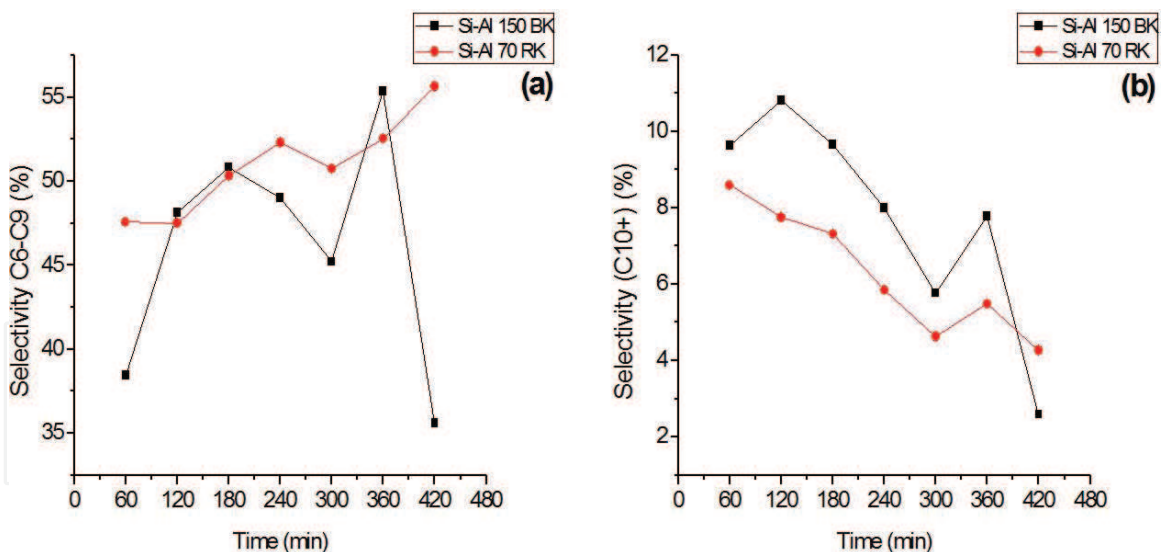


Figure 8.

Selectivity of Si-Al 150 BK and Si-Al 70 RK to gasoline (C_6 – C_9) (a) and diesel (C_{10+}) (b) range products over time on stream.

Both catalysts have a similar trend to selectivity of diesel range products as noticed in the graph and decrease with time as the conversion decreased. However Si-Al 150 BK has a slightly higher selectivity throughout the reaction. Both show good selectivity (40–55%) to gasoline products with the selectivity of Si-Al 70 RK possessing a steady increase over the reaction time. Si-Al 150 BK was more unstable and the selectivity varied over time and was slightly less than Si-Al 70 RK. It was thought Si-Al 70 RK was more selective to reactions pertaining to chain growth such as oligomerisation and alkylation but a closer look at the product selectivity of the gasoline range revealed that Si-Al 70 RK was highly selective to C_6 hydrocarbons as compared to Si-Al 150 BK as shown in **Figure 9**. An increase from ~12% to above 30% was observed. The C_2 – C_5 selectivity trend is also shown and decreases over time for the Si-Al 70 RK catalyst but shows an overall increase in the C_2 – C_5 products

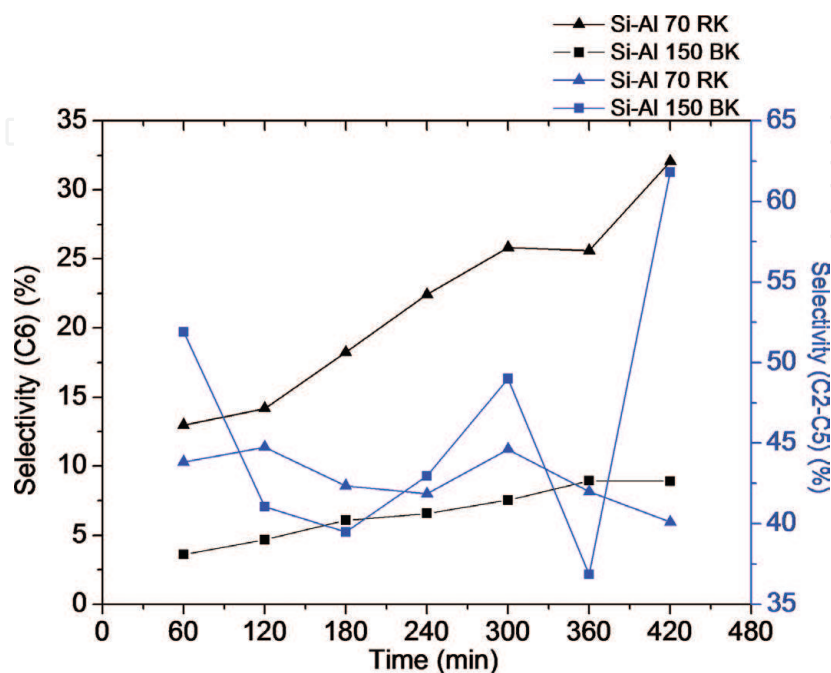


Figure 9.

Selectivity of Si-Al 150 BK and Si-Al 70 RK to C_6 (black curves) and C_2 – C_5 (blue curves) range products over time on stream.

for Si-Al 150 BK. Thus there may be a greater selectivity to isomerisation reactions over cracking reactions for the Si-Al 70 RK catalyst whereas Si-Al 150 BK has a better selectivity to chain growth reactions as its total selectivity to C_{7+} hydrocarbons is higher. This may suggest a slight difference in strength of acid sites available as oligomerisation and cracking occur on stronger acid sites than isomerisation reactions which occur on sites of intermediate acidity [65]. The main difference between the two catalysts however is the crystal morphology and size. The Si-Al 70 RK possessing nanocrystals as shown in HRSEM, this may reduce the effects of diffusion limitation. As shown by Buchanan et al. [66] larger crystals showed a higher selectivity to C_3/C_4 products and a lower isomerization/cracking of olefin ratio due to diffusion limitation. Therefore it is possible that as the strength of the acidic sites are reduced over time due to deactivation which happens more in Si-Al 70 RK, isomerization reactions which occur faster than cracking reactions [66], increase and due to the nanocrystals, the isomers which form are able to diffuse out before any secondary cracking leading to more C_6 isomers, less cracked C_2-C_5 products and a better gasoline selectivity. Therefore the physical properties of the catalyst synthesised from RK are shown to affect its catalytic performance.

Figure 10 shows the selectivity of Si-Al 150 RK, Si-Al 42 RK, Si-Al 70 BK and Si-Al 42 BK to diesel and gasoline range hydrocarbons. The three catalysts with similar conversions i.e. Si-Al 150 RK, Si-Al 42 RK and Si-Al 70 BK can be compared in terms of selectivity.

From **Figure 10** it is noticed that after the first hour on stream the selectivity to C_{10+} is the highest for the catalyst Si-Al 42 RK showing ~16% selectivity. This may indicate that oligomerisation to long chain hydrocarbons largely depends on the acidity since Si-Al 42 RK which has a high Bronsted acidity had the highest selectivity. The more acidic catalysts have better selectivity over the first 3 h on stream. As the reaction proceeds however, all catalysts show a large decrease in selectivity to C_{10+} hydrocarbons except Si-Al 150 RK which shows a greater stability. The decrease for Si-Al 42 RK is almost linear over the reaction time and drops to ~3%. The decrease in selectivity to C_{10+} suggests the deactivation of certain acid sites which are most likely strong Bronsted acid sites as oligomerisation reactions are favoured at these catalytic centres [65]. Si-Al 70 BK which has similar acidity to Si-Al 42 RK shows a slightly better selectivity to C_{10+} hence less deactivation of Bronsted sites. This is most likely due to the higher surface area and increased mesoporosity which may inhibit the build-up of carbonaceous deposits usually responsible for deactivation and hence further highlights the effects of the physicochemical properties of the zeolites on its catalytic behaviour. As mentioned in our previous work [30], the effect of quartz deposits on

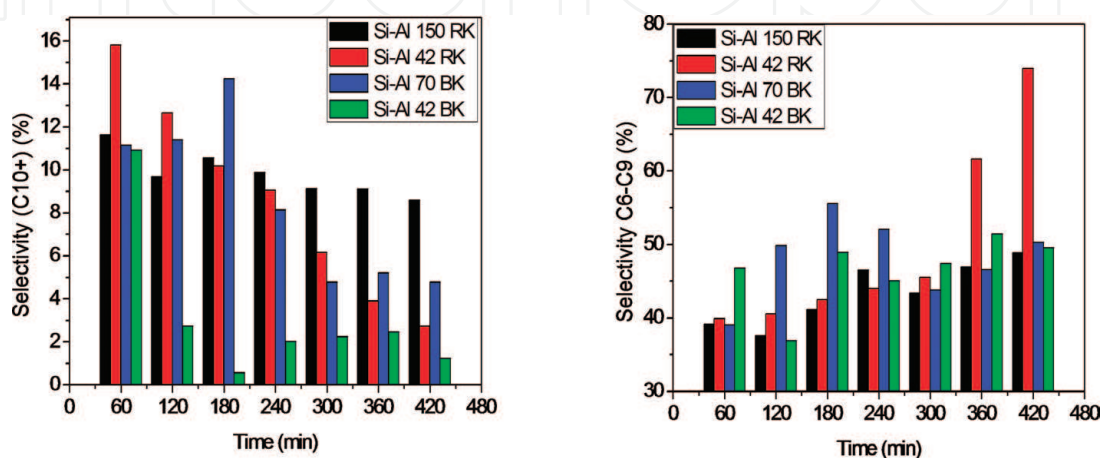


Figure 10. Selectivities to diesel range (C_{10+}) and gasoline range (C_6-C_9) hydrocarbons of catalysts Si-Al 150 RK, Si-Al 42 RK, Si-Al 70 BK and Si-Al 42 BK as a function of time.

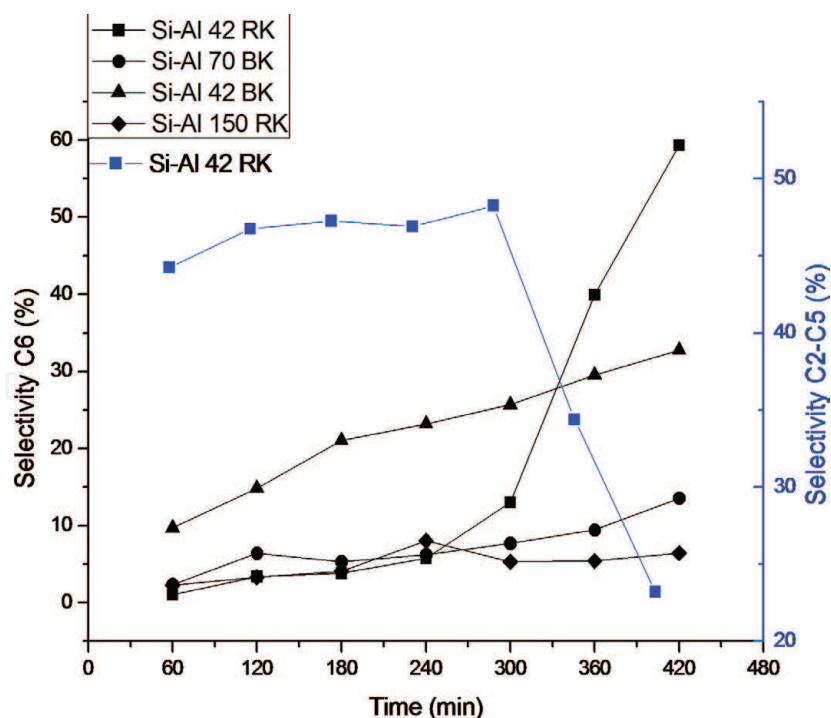


Figure 11. Selectivity to C_6 hydrocarbons and C_2 – C_5 selectivity of Si-Al 42 RK (blue curve) as a function of time.

the external surface of the crystals in Si-Al 150 RK plays a major role in inhibiting the formation of carbonaceous material causing deactivation. Thus even when compared to catalysts with greater acid site density and strength (almost double its acidity), Si-Al 150 RK possesses greater stability and selectivity is almost double that of the more acidic catalysts. This clearly suggests that the acid sites are prevented from being deactivated by the deposition of quartz and continue to catalyse oligomerisation reactions for the duration of the reaction. Si-Al 42 BK had the lowest selectivity to C_{10+} . This is most likely due to its low Bronsted acidity but also the high content of extra-framework aluminium may cause pore blockage and prevent access to acid sites for oligomerisation. The closeness of Al atoms in the structure may also have an effect on the acidity and types of catalytic reactions that are favoured.

All catalysts showed good selectivity to the gasoline range. Si-Al 42 RK shows the opposite trend for selectivity to gasoline as this increase over the reaction time. The selectivity spikes in the last 2 h from 45 to 74%. **Figure 11** shows the selectivity to C_6 and C_2 – C_5 products.

The spike in gasoline activity is again due to an increase in C_6 selectivity. This further confirms our observations with the Si-Al 70 RK catalyst. The decrease in C_{10+} selectivity indicates deactivation of strong acid sites. Thus isomerisation reactions are then favoured when only less acidic sites are available and due to Si-Al 70 RK and Si-Al 42 RK possessing the same morphology the isomerisation products diffuse out before cracking. **Figure 11** clearly shows the contrasting selectivities between isomerisation (C_6) and cracking reactions (C_2 – C_5) for the Si-Al 42 RK catalyst. Si-Al 42 BK also shows good isomerisation activity which further indicates the reaction occurring on weaker acid sites.

4. Conclusion

In conclusion, this chapter discusses some of the key factors affecting the synthesis of kaolin-based ZSM-5 such as kaolin crystallinity, kaolinite content,

crystallisation parameters and Si/Al ratio. Additionally, the catalytic performance of the ZSM-5 derived from kaolin was evaluated. These factors are important considerations when attempting to synthesise ZSM-5 with high purity and crystallinity. However, ZSM-5 can also be synthesised from impure kaolin sources and these impurities may act as poisons or promoters during synthesis and catalytic application. The requirements to develop synthesis conditions that are optimised for specific sources of kaolin are established. The physicochemical properties such as porosity, morphology and acidity of ZSM-5 can be controlled by choosing the right synthesis procedures. Kaolin-based ZSM-5 zeolites are promising as catalysts for petrochemical reactions such as oligomerisation. High activity and selectivity to gasoline and diesel range hydrocarbons was attainable. The activity of the catalysts correlated well with the acidity of ZSM-5 samples. The catalytic performance of the zeolites also correlated well with the physical properties such as morphology and surface area which were shown to influence selectivity to certain products by favouring isomerisation and oligomerisation reactions respectively. Impurities in the kaolin precursor may also have positive effects on catalytic performance, in this case quartz deposition on ZSM-5 inhibiting deactivation and increasing catalyst stability. Therefore, ZSM-5 zeolites can be successfully synthesised from cheaper, more environmentally friendly alternative starting materials that have satisfactory performances in catalytic application.

Acknowledgements

The authors would like to thank the Petroleum, Oil and Gas Corporation of South Africa (PetroSA) for their financial support and technical discussions, the National Research Foundation (NRF) for granting Ebrahim Mohiuddin a scholarship, Makana Brick for supplying the raw kaolin, the electron microscope unit, Physics department, University of the Western Cape for the SEM images, Mrs. E. Antunes, Chemistry department, University of the Western Cape and Dr. D.J. Brand, University of Stellenbosch for the solid state NMR work and Ithemba labs for the XRD work.

IntechOpen

IntechOpen

Author details

Ebrahim Mohiuddin¹, Yusuf Makarfi Isa^{1,2}, Masikana M. Mdleleni^{1*} and David Key¹

1 PetroSA Synthetic Fuels Innovation Centre, South African Institute for Advanced Materials Chemistry, University of the Western Cape, Bellville, South Africa

2 Chemical Engineering Department, Durban University of Technology, Durban, South Africa

*Address all correspondence to: masikana.mdleleni@petrosa.co.za

IntechOpen

© 2018 The Author(s). Licensee IntechOpen. This chapter is distributed under the terms of the Creative Commons Attribution License (<http://creativecommons.org/licenses/by/3.0>), which permits unrestricted use, distribution, and reproduction in any medium, provided the original work is properly cited. 

References

- [1] Chen CY, Zones SI. Post-synthetic treatment and modification of zeolites. In: Cejka J, Avelino C, Stacey Z, editors. *Zeolites and Catalysis: Synthesis, Reactions and Applications*. Weinheim: Wiley-VCH Verlag; 2010. pp. 155-170
- [2] Townsend RP. Ion exchange in zeolites: Some recent developments in theory and practice. *Pure and Applied Chemistry*. 1986;**58**(10):1359-1366
- [3] Ackley M. Application of natural zeolites in the purification and separation of gases. *Microporous and Mesoporous Materials*. 2003;**61**(1-3):25-42
- [4] Weitkamp J. Zeolites and catalysis. *Solid State Ionics*. 2000;**131**:175-188
- [5] Chen NY, Garwood WE. Industrial application of shape-selective catalysis. *Catalysis Reviews*. 1986;**28**(2-3):185-264
- [6] Xiaoning W, Zhen Z, Chunming X, Aijun D, Li Z, Guiyuan J. Effects of light rare earth on acidity and catalytic performance of HZSM-5 zeolite for catalytic cracking of butane to light olefins. *Journal of Rare Earths*. 2007;**25**(20373043):321-328
- [7] De Klerk A. Oligomerization of 1-hexene and 1-octene over solid acid catalysts. *Industrial and Engineering Chemistry Research*. 2005;**44**(11):3887-3893
- [8] Mohiuddin E, Mdleleni MM, Key D. Catalytic cracking of naphtha: The effect of Fe and Cr impregnated ZSM-5 on olefin selectivity. *Applied Petrochemical Research*. 2018;**8**:119
- [9] Aboul-Gheit AK, SM A-H, El-Desouki DS. Catalytic para-xylene maximization. *Applied Catalysis A: General*. 2001;**209**(1-2):179-191
- [10] Abdullahi T, Harun Z, Othman MHD. A review on sustainable synthesis of zeolite from kaolinite resources via hydrothermal process. *Advanced Powder Technology*. 2017;**28**(8):1827-1840
- [11] Yaping Y, Xiaoqiang Z, Weilan Q, Mingwen W. Synthesis of pure zeolites from supersaturated silicon and aluminum alkali extracts from fused coal fly ash. *Fuel*. 2008;**87**(10-11):1880-1886
- [12] Kordatos K, Gavela S, Ntziouni a, Pistiolas KN, Kyritsi a, Kasselouri-Rigopoulou V. Synthesis of highly siliceous ZSM-5 zeolite using silica from rice husk ash. *Microporous and Mesoporous Materials*. 2008;**115**(1-2):189-196
- [13] Mohamed MM, Zidan FI, Thabet M. Synthesis of ZSM-5 zeolite from rice husk ash: Characterization and implications for photocatalytic degradation catalysts. *Microporous and Mesoporous Materials*. 2008;**108**(1-3):193-203
- [14] Panpa W, Jinawath S. Synthesis of ZSM-5 zeolite and silicalite from rice husk ash. *Applied Catalysis B: Environmental*. 2009;**90**:389-394
- [15] Wang P, Shen B, Shen D, Peng T, Gao J. Synthesis of ZSM-5 zeolite from expanded perlite/kaolin and its catalytic performance for FCC naphtha aromatization. *Catalysis Communications*. 2007;**8**(10):1452-1456
- [16] Jiang J, Duanmu C, Yang Y, Gu X, Chen J. Synthesis and characterization of high siliceous ZSM-5 zeolite from acid-treated palygorskite. *Powder Technology*. 2014;**251**:9-14
- [17] Chareonpanich M, Namto T, Kongkachuichay P, Limtrakul J.

Synthesis of ZSM-5 zeolite from lignite fly ash and rice husk ash. *Fuel Processing Technology*. 2004;**85**(15):1623-1634

[18] Feng H, Li C, Shan H. Effect of calcination temperature of kaolin microspheres on the In situ synthesis of ZSM-5. *Catalysis Letters*. 2008;**129**(1-2):71-78

[19] Khatamian M. Preparation and characterization of nanosized ZSM-5 zeolite using kaolin and investigation of kaolin content, crystallization time and temperature changes on the size and crystallinity of products. *Journal of the Iranian Chemical Society*. 2009;**6**(1):187-194

[20] Kovo AS, Hernandez O, Holmes SM. Synthesis and characterization of zeolite Y and ZSM-5 from Nigerian Ahoko Kaolin using a novel, lower temperature, metakaolinization technique. *Journal of Materials Chemistry*. 2009;**19**(34):6207-6212

[21] Pan F, Lu X, Wang Y, Chen S, Wang T, Yan Y. Organic template-free synthesis of ZSM-5 zeolite from coal-series kaolinite. *Materials Letters*. 2014;**115**(1):5-8

[22] Gualtieri A, Norby P, Artioli G, Hanson J. Kinetics of formation of zeolite Na-A [LTA] from natural kaolinites. *Physics and Chemistry of Minerals*. 1997;**24**:191-199

[23] Murat M, Amokrane A, Bastide J, Montanaro L. Synthesis of zeolites from thermally activated kaolinite. Some observations on nucleation and growth. *Clay Minerals*. 1992;**27**(1):119-130

[24] Shirazi L, Jamshidi E, Ghasemi MR. The effect of Si/Al ratio of ZSM-5 zeolite on its morphology, acidity and crystal size. *Crystal Research and Technology*. 2008;**43**(12):1300-1306

[25] Caballero I, Colina FG, Costa J. Synthesis of X-type zeolite from dealuminated kaolin by reaction with sulfuric acid at high temperature. *Industrial and Engineering Chemistry Research*. 2007;**46**(4):1029-1038

[26] Lafi AAF, Matam SK, Hodali HA. New synthesis of ZSM-5 from high silica kaolinite and its use in vapor phase conversion of 1-phenylethanol to styrene new synthesis of ZSM-5 from high silica kaolinite and its use in vapor phase conversion of 1-phenylethanol to styrene. *Industrial and Engineering Chemistry Research*. 2015;**54**(15):3754-3760

[27] Bergaya F, Lagaly G. Chapter 1: General introduction: Clays, clay minerals, and clay science. In: *Developments in Clay Science*. Netherlands: Elsevier B.V. 2006. pp. 1-18

[28] Bloodworth AJ, Highley DE, Mitchell CJ. *Industrial Minerals Laboratory Manual: Kaolin*. BGS Technical Report WG/93/1, 2014. 1993

[29] Barrer RM. *Hydrothermal Chemistry of Zeolites*. London, New York: Academic Press; 1982

[30] Mohiuddin E, Isa YM, Mdleleni MM, Sincadu N, Key D, Tshabalala T. Synthesis of ZSM-5 from impure and beneficiated Grahamstown kaolin: Effect of kaolinite content, crystallisation temperatures and time. *Applied Clay Science*. 2016;**119**:213-221

[31] Belviso C, Cavalcante F, Lettino A, Fiore S. A and X-type zeolites synthesised from kaolinite at low temperature. *Applied Clay Science*. 2013;**80-81**:162-168

[32] Chandrasekhar S. Influence of metakaolinization temperature on the formation of zeolite 4A from kaolin. *Clay Minerals*. 1996;**31**(2):253-261

- [33] Granizo ML, Blanco-Varela MT, Palomo A. Influence of the starting kaolin on alkali-activated materials based on metakaolin. Study of the reaction parameters by isothermal conduction calorimetry. *Journal of Materials Science*. 2000;**35**(24):6309-6315
- [34] Johnson EBG, Arshad SE. Hydrothermally synthesized zeolites based on kaolinite: A review. *Applied Clay Science*. 2014;**97-98**:215-221
- [35] Mohiuddin E, Isa YM, Mdleleni MM, Key D. Effect of kaolin chemical reactivity on the formation of ZSM-5 and its physicochemical properties. *Microporous and Mesoporous Materials*. 2017:237
- [36] Chandrasekhar S, Pramada PN. Microwave assisted synthesis of zeolite A from metakaolin. *Microporous and Mesoporous Materials*. 2008;**108**(1-3):152-161
- [37] Dedecek J, Balgová V, Pashkova V, Klein P, Wichterlová B. Synthesis of ZSM-5 zeolites with defined distribution of Al atoms in the framework and multinuclear MAS NMR analysis of the control of Al distribution. *Chemistry of Materials*. 2012;**24**:3231-3239
- [38] Maia AÁB, Angélica RS, de Freitas Neves R, Pöllmann H, Straub C, Saalwächter K. Use of ²⁹Si and ²⁷Al MAS NMR to study thermal activation of kaolinites from Brazilian Amazon kaolin wastes. *Applied Clay Science*. 2014;**87**:189-196
- [39] Magusin PCMM, Zorin VE, Aerts A, Houssin CJY, Yakovlev AL, Kirschhock CEA, et al. Template-aluminosilicate structures at the early stages of zeolite ZSM-5 formation. A combined preparative, solid-state NMR, and computational study. *The Journal of Physical Chemistry. B*. 2005;**109**(48):22767-22774
- [40] Eilertsen EA, Haouas M, Pinar AB, Hould ND, Lobo RF, Lillerud KP, et al. NMR and SAXS analysis of connectivity of aluminum and silicon atoms in the clear sol precursor of SSZ-13 zeolite. *Chemistry of Materials*. 2012;**24**:571-578
- [41] Murray LJ, Heckrodt RO. South African kaolins. In: *International Clay Conference*. 1978. pp. 601-608
- [42] Saikia NJ, Bharali DJ, Sengupta P, Bordoloi D, Goswamee RL, Saikia PC, et al. Characterization, beneficiation and utilization of a kaolinite clay from Assam, India. *Applied Clay Science*. 2003;**24**(1-2):93-103
- [43] Panda AK, Mishra BG, Mishra DK, Singh RK. Effect of sulphuric acid treatment on the physico-chemical characteristics of kaolin clay. *Colloids and Surfaces A: Physicochemical and Engineering Aspects*. 2010;**363**(1-3):98-104
- [44] Holmes SM, Alomair AA, Kovo AS. The direct synthesis of pure zeolite-A using “virgin” kaolin. *RSC Advances*. 2012;**2**(30):11491
- [45] Velho JAGL, SF GC d. Characterization of Portuguese kaolins for the paper industry: Beneficiation through new delamination techniques. *Applied Clay Science*. 1991;**6**(2):155-170
- [46] Mignoni ML, Petkowicz DI, Fernandes Machado NRC, Pergher SBC. Synthesis of mordenite using kaolin as Si and Al source. *Applied Clay Science*. 2008;**41**(1-2):99-104
- [47] Yu J. Synthesis of zeolites. In: Cejka J, van Bekkum H, Corma A, Schuth F, editors. *Introduction to Zeolite Science and Practice*. 3rd Revised ed. Netherlands: Elsevier B.V. 2007. pp. 39-103
- [48] Kovo SA. Development of zeolites and zeolite membranes from Ahoko Nigerian Kaolin. [doctoral thesis].

England: The University of Manchester; 2011

[49] Na J, Liu G, Zhou T, Ding G, Hu S, Wang L. Synthesis and catalytic performance of ZSM-5/MCM-41 zeolites with varying mesopore size by surfactant-directed recrystallization. *Catalysis Letters*. 2013;**143**(3):267-275

[50] Liu C, Kong D, Guo H. The morphology control of zeolite ZSM-5 by regulating the polymerization degree of silicon and aluminum sources. *Microporous and Mesoporous Materials*. 2014;**193**:61-68

[51] Gobin OC, Reitmeier SJ, Jentys A, Lercher JA. Comparison of the transport of aromatic compounds in small and large MFI particles. *Journal of Physical Chemistry C*. 2009;**113**(47):20435-20444

[52] Zhang R, Zhang B, Shi Z, Liu N, Chen B. Catalytic behaviors of chloromethane combustion over the metal-modified ZSM-5 zeolites with diverse SiO₂/Al₂O₃ ratios. *Journal of Molecular Catalysis A: Chemical*. 2015;**398**:223-230

[53] Serrano DP, García RA, Vicente G, Linares M, Procházková D, Čejka J. Acidic and catalytic properties of hierarchical zeolites and hybrid ordered mesoporous materials assembled from MFI protozeolitic units. *Journal of Catalysis*. 2011;**279**(2):366-380

[54] Wang S, Dou T, Li Y, Zhang Y, Li X, Yan Z. A novel method for the preparation of MOR/MCM-41 composite molecular sieve. *Catalysis Communications*. 2005;**6**(1):87-91

[55] Tang Q, Xu H, Zheng Y, Wang J, Li H, Zhang J. Catalytic dehydration of methanol to dimethyl ether over micro-mesoporous ZSM-5/MCM-41 composite molecular sieves. *Applied Catalysis A: General*. 2012;**413-414**:36-42

[56] Yang ZX, Xia YD, Mokaya R. Zeolite ZSM-5 with unique supermicropores synthesized using mesoporous carbon as a template. *Advanced Materials*. 2004;**16**(8):727-732

[57] Groen JC, Peffer LAA, Pérez-Ramírez J. Pore size determination in modified micro- and mesoporous materials. Pitfalls and limitations in gas adsorption data analysis. *Microporous and Mesoporous Materials*. 2003;**60**(1-3):1-17

[58] Yue Y, Liu H, Yuan P, Li T, Yu C, Bi H, et al. From natural aluminosilicate minerals to hierarchical ZSM-5 zeolites: A nanoscale depolymerization-reorganization approach. *Journal of Catalysis*. 2014;**319**:200-210

[59] Rodríguez-González L, Hermes F, Bertmer M, Rodríguez-Castellón E, Jiménez-López A, Simon U. The acid properties of H-ZSM-5 as studied by NH₃-TPD and ²⁷Al-MAS-NMR spectroscopy. *Applied Catalysis A: General*. 2007;**328**(2):174-182

[60] Cabral de Menezes SM, Lam YL, Damodaran K, Pruski M. Modification of H-ZSM-5 zeolites with phosphorus. 1. Identification of aluminum species by ²⁷Al solid-state NMR and characterization of their catalytic properties. *Microporous and Mesoporous Materials*. 2006;**95**(1-3):286-295

[61] Woolery GL, Kuehl GH, Timken HC, Chester a W, Vartuli JC. On the nature of framework Brønsted and Lewis acid sites in ZSM-5. *Zeolites*. 1997;**19**(4):288-296

[62] Oldfield E, Haase J, Schmitt KD, Schramm SE. Characterization of zeolites and amorphous silica—Aluminas by means of aluminum-27 nuclear magnetic resonance spectroscopy: A multifold, multiparameter investigation. *Zeolites*. 1994;**14**(2):101-109

[63] Prasad JV, Rao KV, Bhat YS, Halgeri AB. MAS NMR studies of ZSM-5 zeolites: Correlation to para selectivity and SEM observations. *Catalysis Letters*. 1992;**14**(3-4):349-357

[64] Smaïhi M, Barida O, Valtchev V. Investigation of the crystallization stages of LTA-type zeolite by complementary characterization techniques. *European Journal of Inorganic Chemistry*. 2003;**24**:4370-4377

[65] Van Donk S, Bitter JH, De Jong KP. Deactivation of solid acid catalysts for butene skeletal isomerisation: On the beneficial and harmful effects of carbonaceous deposits. *Applied Catalysis A: General*. 2001;**212**(1-2):97-116

[66] Buchanan JS, Olson DH, Schramm SE. Gasoline selective ZSM-5 FCC additives: Effects of crystal size, SiO₂/Al₂O₃, steaming, and other treatments on ZSM-5 diffusivity and selectivity in cracking of hexene/octene feed. *Applied Catalysis A: General*. 2001;**220**(1-2):223-234